Premelting-Induced Smoothening of the Ice-Vapor Interface

Jorge Benet,* Pablo Llombart, Eduardo Sanz, and Luis G. MacDowell†
Departamento de Química-Física, Facultad de Ciencias Químicas, Universidad Complutense de Madrid, 28040 Madrid, Spain
(Received 21 August 2015; revised manuscript received 22 July 2016; published 24 August 2016)

We perform computer simulations of the quasiliquid layer of ice formed at the ice-vapor interface close to the ice Ih-liquid-vapor triple point of water. Our study shows that the two distinct surfaces bounding the film behave at small wavelengths as atomically rough and independent ice-water and water-vapor interfaces. For long wavelengths, however, the two surfaces couple, large scale parallel fluctuations are inhibited, and the ice-vapor interface becomes smooth. Our results could help explain the complex morphology of ice crystallites.

DOI: 10.1103/PhysRevLett.117.096101

Nakaya summarized his research on snow flakes in a famous *haiku*: "They are letters sent to us from the sky" [1]. Indeed, the habit of ice crystals grown from bulk vapor change from plates, to columns, to plates, and yet back to columns as the temperature is cooled down below the triple point, with the well known dendritic patterns appearing at sufficiently high supersaturations [2]. Accordingly, the final growth form of a tiny ice crystal conveys detailed information on the atmosphere where it grew [3].

At a macroscopic level, it is well known that changes in ice crystal habits result from a crossover in the growth rates of the basal and prismatic faces, but exactly what structural transformations occur on the surface to drive this crossover is far from being understood [1,2,4,5]. Kuroda and Lacmann explained the crossover in crystal growth rates as a result of the formation of a thin quasiliquid layer on the ice surface that could set up at different temperatures depending on the crystal facet [6].

The hypothesis that ice could exhibit a quasiliquid layer dates back to Faraday, and the formation of such a layer on solid surfaces is now well characterized theoretically as a premelting surface phase transition [7]. Experimentally, the advent of modern optical and surface scattering techniques has allowed us to gather ample evidence as regards the existence of a premelting liquid film on the surface of ice [8–14]. Unfortunately, the relatively high vapor pressure of ice makes it very difficult to achieve sizable equilibrium crystals [2], while the presence of impurities has a very large impact on the surface structure [12,15]. Accordingly, many other relevant properties, such as the premelting temperature, the thickness of the quasiliquid layer, or the presence of surface melting remain a matter of debate [8].

One particularly important structural property with a large impact on crystal growth rates is the surface roughness [6,16,17]. Contrary to smooth or singular facets, which have a limited number of defects and serve as the basis for most crystal growth models, rough surfaces present diverging height fluctuations, which do not differ macroscopically from those found in a fluid interface. As a result, rough crystal planes with correlation lengths that are larger than the crystallite disappear and become round [18–20]. More importantly, as far as the crystal habits and growth forms are concerned, the roughening of a surface has dramatic consequences on the dynamics, as it signals a crossover from a two-dimensional nucleated growth, to a faster Knudsen mechanism that is linear in the saturation [6,17]. Unfortunately, this phenomenology has been established only for rather simple interfaces [17], and the role of a premelting film in the surface roughness is largely unknown.

Here, we perform computer simulations of a premelting layer on the primary prismatic facet of the ice-vapor interface. Our study reveals that the structure and fluctuations of the surfaces bounding the quasiliquid layer at small length scales are very much like those of atomically rough and independent ice-water and water-vapor interfaces. However, the finite equilibrium thickness of the premelting layer below the triple point drives the long-wavelength structure of the interface from rough to smooth. Our results clarify why the facets of ice crystals remain recognizable up to the triple point, and suggest the formation of a premelting layer could slow down the growth kinetics, as required to explain ice crystal growth habits in the atmosphere [6].

Our study is performed with the TIP4P/2005 model of water [21], which has been shown to reproduce with remarkable accuracy a large number of bulk and surface properties of (liquid) water and ice [22]. A slab of equilibrated bulk ice with several thousand molecules is placed in contact with vacuum inside a large orthorhombic simulation box, such that an interface of surface area $A = L_x L_y$ is exposed parallel to the xy plane. The surfaces thus prepared exhibit a very large heterogeneity of vacancy energies, with a strong dependence on the proton ordering arrangements [23]. For this reason we prepare our initial samples using a special purpose Monte Carlo algorithm that suitably samples the hydrogen bond network [24–26]. Averages are then collected using molecular dynamics with the GROMACS package for about half a microsecond [27–35], well above

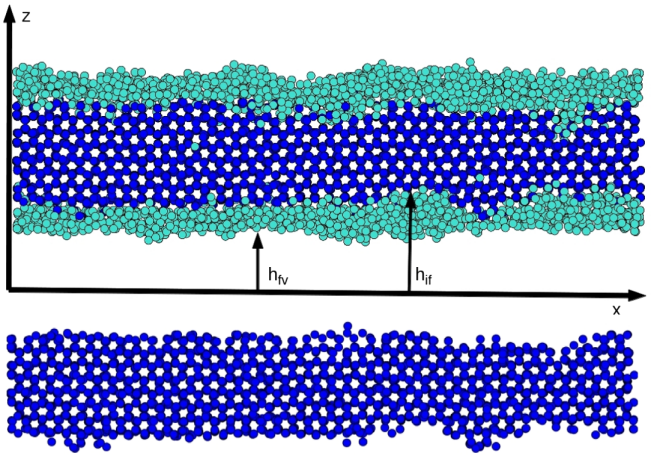

FIG. 1. Snapshot of the ice-vapor interface during the course of our simulations. Top: a quasiliquid layer of disordered molecules is clearly seen on top of the bulk ice. The order parameter allows us to distinguish between an ice-film and a film-vapor surface. Bottom: same figure with the liquidlike atoms removed.

the expected relaxation time for the ice-water interface [36]. Performing the simulations along the sublimation line at a temperature just $\Delta T = T - T_t = 2$ K below the triple point temperature T_t, [37] the first few ice layers melt and form a premelting quasiliquid layer (Fig. 1), as noticed earlier [38–41]. The nature and size of this layer may be quantified using the $\bar{q}_6$ order parameter [42], which has been optimized to discriminate icelike and waterlike molecules from a study of molecular correlations up to second nearest neighbors [43]. To get rid of the vapor molecules, we identify the premelting layer as the largest cluster of water molecules, and find an average thickness of $\ell = 0.9$ nm, in reasonable agreement with experimental observations [12,14], and recent simulations [38–40]. Here, we attempt to characterize the quasiliquid film in terms of two fluctuating ice-film and film-vapor surfaces, which we locate by locally averaging the heights of the outermost solid and liquid molecules of the layer, respectively (Fig. 1). Comparing our results for the ice-vapor interface with our previous study of the ice-water interface will prove insightful [44]. Since we aim at studying large wavelength fluctuations, we prepare the exposed faces with an elongated geometry, with box side $L_x \gg L_y$. This allows us to identify ice-film $h_{\rm if}(x)$ and film-vapor $h_{\rm fv}(x)$ surface profiles along the largest axis x. These film profiles are then Fourier transformed to yield the spectrum of surface fluctuations [27].

For the purpose of studying the fluctuations of the quasiliquid layer, it is convenient to define the quantity $\Gamma_{\alpha\beta}(q_x)$, in terms of the thermal averages of Fourier amplitudes $h_{\alpha\beta}$, as

$$\Gamma_{\alpha\beta}(q_x) = \frac{k_B T}{A\langle h_{\alpha\beta}(q_x) h^*_{\alpha\beta}(q_x)\rangle q_x^2}, \qquad (1)$$

where k_B is Boltzmann's constant, $q_x = 2\pi n/L_x$, and n is a positive integer. According to capillary wave theory [45], for a rough interface between bulk phases α and β, the function $\Gamma_{\alpha\beta}(q_x)$ may be identified with a wave-vector dependent stiffness $\tilde{\gamma}_{\alpha\beta}(q_x)$ whose $q_x \to 0$ limit is the macroscopic stiffness of the interface [46–48], corresponding exactly to the surface tension for fluid-fluid interfaces [49,50]. In the forthcoming exposition we concentrate on the primary prismatic plane (pI) at $\Delta T = -2$ K and study the fluctuations propagated along the basal [basal] and secondary prismatic [pII] directions.

The results $\Gamma_{\rm if}(q_x)$ and $\Gamma_{\rm fv}(q_x)$ obtained for the ice-film and film-vapor surface fluctuations of the premelting layer on the primary prismatic plane, either along the [basal] or [pII] orientations, agree very nicely with those obtained for the corresponding ice-water, $\Gamma_{\rm iw}(q_x)$, and water-vapor, $\Gamma_{\rm wv}(q_x)$, interfaces down to $q_x^* = 1.5$ nm^{-1} [Figs. 2(a) and 2(b)]. This implies that for a quasiliquid layer hardly 1 nm thick, the ice-film and film-vapor surfaces at this length scale fluctuate independently, with fluctuations that can hardly be distinguished from those found at the rough interfaces of bulk water. Interestingly, at $q_x \approx q_x^*$, $\Gamma_{\rm iw}(q_x)$ and $\Gamma_{\rm wv}(q_x)$ are already close to their $q_x \to 0$ limit, and are therefore close to the corresponding macroscopic stiffness coefficients.

The striking resemblance between the surface fluctuations of the quasiliquid layer and bulk water for $q_x > q_x^*$ can be understood in terms of the density profiles shown in Fig. 3 for the primary prismatic plane (with similar results found for the basal and secondary prismatic planes, cf. Ref. [27]). Indeed, the density profile of the solidlike molecules from the ice-vapor interface (full red) almost matches that observed at the ice-water interface (dashed indigo). Similarly, the profile of the liquidlike molecules of the quasiliquid layer at the ice-vapor interface (full blue) is very similar to that at the ice-water interface (dashed green) until the very end of the premelting film, where it obviously drops to the values expected for the bulk vapor density.

Below q_x^*, the fluctuating surfaces start noticing the finite thickness of the quasiliquid layer, as implied by the departure of $\Gamma_{\rm if}(q_x)$ and $\Gamma_{\rm fv}(q_x)$ from the ice-water and water-vapor behavior. For the fluctuations in the (pI)[pII] direction, a sharp rise of $\Gamma(q_x)$ for both the ice-film and film-vapor surfaces suggests a divergence as $q_x \to 0$, and indicates the onset of a completely different regime, with finite correlations at infinite wavelengths and an effective infinite stiffness coefficient [Fig. 2(a)]. For the fluctuations in the (pI)[basal] direction, on the contrary, $\Gamma(q_x)$ rises above the values expected for the ice-water and water-vapor interfaces, but seems to attain a finite asymptotic limit for $q_x \to 0$ [Fig. 2(b)]. These conflicting results for the (pI) interface at $\Delta T = -2$ K indicate the proximity of a roughening transition, where the interface depins from the underlying bulk solid. Roughening is a Kosterlitz-Thouless transition of infinite order [20]. Not unexpectedly,

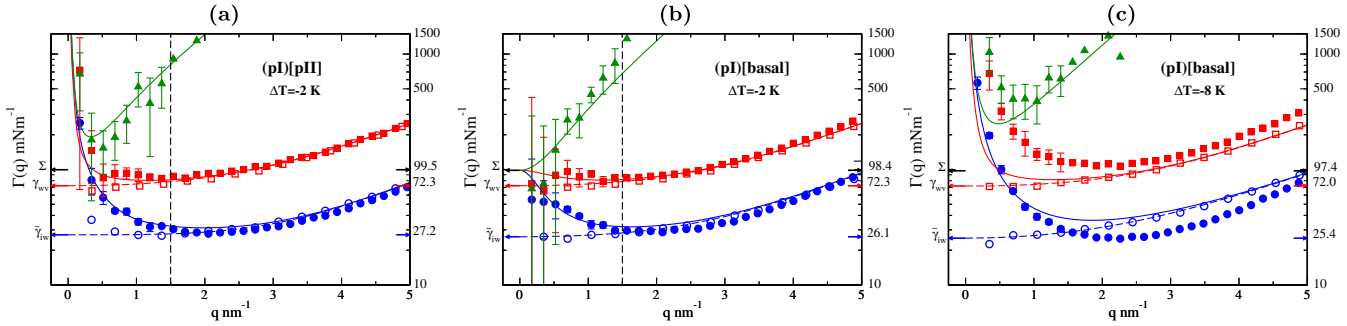

FIG. 2. Fluctuations of the premelting film on the primary prismatic plane. The plot displays the effective wave-vector dependent stiffness $\Gamma(q_x)$ in log scale for (pI)[pII] at $\Delta T = -2$ K (a), and (pI)[basal] at $\Delta T = -2$ K (b) and $\Delta T = -8$ K (c). Results for the quasiliquid layer are shown with filled symbols, with $\Gamma_{\rm if}(q_x)$ for the ice-film (blue circles) and $\Gamma_{\rm fv}(q_x)$ for the film-vapor surfaces (red squares). The open symbols are the results for the ice-water (blue circles) and water-vapor (red squares) interfaces, which are fitted to $\Gamma(q_x) = \gamma + \kappa q_x^2 + \epsilon q_x^4$ (dashed lines) for the purpose of extrapolation (cf. Refs. [44] and [27]). The colored arrows indicate the extrapolation to $q_x = 0$, which provides the ice-water stiffness $\tilde{\gamma}_{\rm iw}$ and the water-vapor surface tension $\gamma_{\rm wv}$, respectively. The black arrow points to $\Sigma = \tilde{\gamma}_{\rm iw} + \gamma_{\rm wv}$, where the effective stiffness of the quasiliquid film would converge were the interface rough. The dashed vertical line indicates approximately the regime of q_x where the quasiliquid surfaces cease to behave independently. The green triangles indicate the results for the coupled fluctuations of the ice-film and film-vapor surfaces, $\Gamma_{\rm iv}(q_x)$. The full lines are the results from a fit to the model of Eq. (4).

the error bars observed for $\Gamma(q_x)$ are extremely large, and subaverages may be collected, which appear consistent with either a rough or a smooth interface. By simulating the same interfaces just 6 K below, we find that $\Gamma(q_x)$ also becomes divergent for the (pI)[basal] direction, confirming the smoothening of the interface just a few degrees kelvin below the triple point (as expected the divergence remains for the (pI)[pII] direction. cf. Ref. [27]). This result is consistent with the rounding of the edges between prismatic facets observed in simulations of ice microcrytallites [40].

The observation of a roughening transition at about $\Delta T = -2$ K is somewhat puzzling. Given the similarity between the structure of the quasiliquid layer and bulk water at short length scales, why are the long wavelength fluctuations so different? Here, we show how the finite thickness of the premelting film can change completely the low wave-vector response of the ice-film and film-vapor surfaces even under the assumption that the corresponding stiffness coefficients are exactly those of the rough ice-water and water-vapor interfaces, respectively.

To see this, we consider the sine-Gordon model of the solid-liquid interface [20,45], and assume that the free energy of the ice-film layer is given solely in terms of parameters akin to the ice-water interface:

$$H_{\rm if} = \int d\mathbf{x} \left(\frac{1}{2} \tilde{\gamma}_{\rm iw} (\nabla h_{\rm if})^2 - u \cos(k_z h_{\rm if}) \right), \qquad (2)$$

where $\tilde{\gamma}_{\rm iw}$ is the interface stiffness, $k_z = (2\pi/b)$, and b is the interplane spacing. In this model, the square gradient term penalizes the departure of the ice-film layer from planarity, while the cosine term favors by an amount u those configurations where $h_{\rm if}(\mathbf{x})$ is a multiple of the lattice spacing. For the film-vapor surface, we consider that the free energy is described by capillary wave theory, with departures from planarity penalized by the water-vapor surface tension $\gamma_{\rm wv}$ [51]:

$$H_{\rm fv} = \int d\mathbf{x} \left(\frac{1}{2} \gamma_{\rm wv} (\nabla h_{\rm fv})^2 + g(\Delta h) \right). \qquad (3)$$

For an inert substrate, $g(\Delta h)$ is the interface potential, which dictates the free energy of a planar premelting film of height Δh [52]. In our model, it plays the crucial role of coupling the film-vapor fluctuations to the ice-film surface, since $\Delta h = h_{\rm fv} - h_{\rm if}$.

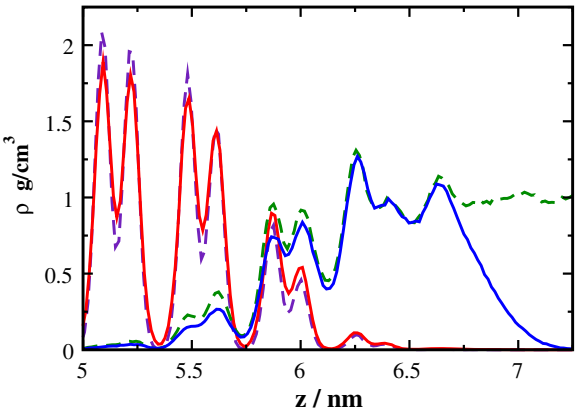

FIG. 3. Structure of the ice-vapor (full lines) and ice-liquid (dashed lines) interfaces of the primary prismatic plane along the perpendicular direction. The density of the solidlike molecules is shown in full red for the solid-vapor interface and in dashed indigo for the solid-liquid interface. The density of the liquidlike molecules is shown in full blue for the solid-vapor interface and in dashed green for the solid-liquid interface.

To solve for this coupled capillary wave + sine-Gordon model approximately, we extend a variational theory for the sine-Gordon model due to Safran [45]. The solution yields the Fourier modes of the surface fluctuations, as follows [27]:

$$\begin{aligned}\langle|h_{\rm if}^2(q_x)|\rangle &= \frac{k_BT}{A}\frac{g''+\gamma_{\rm wv}q_x^2}{wg''+(g''\Sigma+w\gamma_{\rm wv})q_x^2+\gamma^2q_x^4},\\ \langle|h_{\rm fv}^2(q_x)|\rangle &= \frac{k_BT}{A}\frac{w+g''+\tilde{\gamma}_{\rm iw}q_x^2}{wg''+(g''\Sigma+w\gamma_{\rm wv})q_x^2+\gamma^2q_x^4},\\ \langle h_{\rm if}(q_x)h_{\rm fv}^*(q_x)\rangle &= \frac{k_BT}{A}\frac{g''}{wg''+(g''\Sigma+w\gamma_{\rm wv})q_x^2+\gamma^2q_x^4},\end{aligned} \tag{4}$$

where g'' is the second derivative of the interface potential with respect to the layer thickness, $\Sigma=\tilde{\gamma}_{\rm iw}+\gamma_{\rm wv}$, and $\gamma^2=\tilde{\gamma}_{\rm iw}\gamma_{\rm wv}$, while w is a roughness parameter that needs to be solved self-consistently:

$$w = uk_z^2 e^{-\frac{1}{2}k_z^2\sum_{\mathbf{q}}\langle|h_{\rm if}^2(\mathbf{q})|\rangle}. \tag{5}$$

Notice that the sum over the wave vectors confers to w a dependence on the surface geometry [27].

The above result nicely rationalizes our observations. At large wave vectors, $q\to\infty$, the system is atomically rough, i.e., $\Gamma_{\rm if}(q_x)\to\tilde{\gamma}_{\rm iw}$ and $\Gamma_{\rm fv}(q_x)\to\gamma_{\rm wv}$, whence the ice-film and film-vapor surfaces behave as rough ice-water and water-vapor interfaces as observed in Figs. 2(a) and 2(b).

Furthermore, the fluctuations are then fully independent. This can be seen by considering the cross correlations $\langle h_{\rm if}(q_x)h_{\rm fv}^*(q_x)\rangle$, which in this limit fall to zero. Defining the related function $\Gamma_{\rm iv}(q_x)=k_BT/A\langle h_{\rm if}(q_x)h_{\rm fv}^*(q_x)\rangle q_x^2$, consistent with Eq. (1), we find indeed that our simulation results for $\Gamma_{\rm iv}(q_x)$ diverge at large q (see Fig. 2). This regime of large wave vectors is consistent with the observations by Limmer and Chandler, who measured a stiffness coefficient from the ice-film fluctuations in reasonable agreement with results for the ice-liquid interface in their simulations [41]. In the limit of small wave vectors, $q_x\to 0$, however, we get qualitatively different behaviors depending on the roughness parameter (cf. Fig. 6 of Ref. [27]). On the one hand, if $w=0$, the fluctuations diverge, and both surfaces behave as rough interfaces with stiffness Σ, [i.e., $\Gamma_{\rm if}(0)=\Gamma_{\rm fv}(0)=\Gamma_{\rm iv}(0)=\Sigma$]. On the other hand, if $w\neq 0$, the fluctuations remain finite as $q_x\to 0$, whence $\Gamma_{\alpha\beta}(q_x)$ diverges as q_x^{-2}, indicating a smooth interface. Despite the atomic roughness at small length scales, the smoothening of the surface has dramatic consequences, since both the crystal shape and crystal growth rate are dictated by $\Gamma_{\rm if}(\mathbf{q}\to 0)$ [17–19,45].

In our simulations at $\Delta T=-2$ K, we observe, for the (pI)[basal] direction, a behavior consistent with $w=0$, corresponding to a rough interface [Fig. 2(b)]. For the (pI)[pII] direction, on the contrary, we clearly observe for the smallest wave vector accessible that $\Gamma_{\rm fv}(q_x)$ has largely exceeded Σ, while $\Gamma_{\rm iv}(q_x)$ attains a minimum well above Σ, and then exhibits a strong divergence, as predicted by our model for a smooth interface [Fig. 2(a)]. This "roughness anisotropy" is consistent with Eq. (5), which indicates that the roughening temperature for the (pI)[pII] direction could be higher than that of the (pI)[basal] direction by a factor $\approx$1.01 given by the ratio of the ice-vapor stiffness coefficients (Σ) [27].

The qualitative statements that result from our model may be made quantitative and may be extended to large wave vectors provided we replace $\tilde{\gamma}_{\rm iw}$ and $\gamma_{\rm wv}$ in Eq. (4) by the phenomenological wave-vector dependent coefficients $\tilde{\gamma}_{\rm iw}(q_x)$, and $\gamma_{\rm wv}(q_x)$ obtained from the simulations of the ice-water and water-vapor interfaces. A least square fit to the Fourier amplitudes of (pI) at $\Delta T=-2$ K yields $g''\approx 8\times 10^{15}$ J/m^4 for both directions, while the roughness parameter is $w=0$ for the (pI)[basal] direction and $w=3.3\times 10^{15}$ J/m^4 for the (pI)[pII] direction, indicative of the proximity of a roughening transition. At $\Delta T=-8$ K, the fit for both directions is consistent with $g''\approx 12\times 10^{15}$ J/m^4 and $w\approx 8\times 10^{15}$ J/m^4, corresponding to a smooth interface.

But how can the surface of the ice-film interface become smooth for small wave vectors while the small wavelength structure remains essentially equal to that of a film of infinite depth? This question can be answered by solving for the self-consistent condition Eq. (5), with the help of Eq. (4). The result gives w as the root of a transcendental equation [27]. For a film of infinite height, with $g''=0$, we obtain

$$w \propto \left(1+\frac{\tilde{\gamma}_{\rm iw}}{w}q_{\rm max}^2\right)^{-\tau_{\rm iw}}, \tag{6}$$

where $q_{\rm max}$ is an upper wave-vector cutoff for the fluctuations. The above result corresponds to the approximate solution of the sine-Gordon model due to Safran [45]. The resulting transcendental equation depends essentially on one parameter: $\tau_{\rm iw}=(k_BTk_z^2/8\pi\tilde{\gamma}_{\rm iw})$. For $\tau_{\rm iw}>1$, the root is $w=0$, and the surface is rough, while for $\tau_{\rm iw}<1$, the root is finite, and the surface is smooth. For films of finite depth, $g''>0$, and the situation changes. The roots are still governed by an equation similar to the above result,

$$w \propto \left(1+\frac{\Sigma}{w}q_{\rm max}^2\right)^{-\mu_{\rm if}}, \tag{7}$$

but now the exponent is $\mu_{\rm if}=(\tilde{\gamma}_{\rm iw}/\Sigma)\times\tau_{\rm iw}$, which is always smaller than $\tau_{\rm iw}$ [27]. Hence, for a rough ice-water surface with $\tau_{\rm iw}$ close but greater than unity, $\mu_{\rm if}$ will be much smaller than unity, and the corresponding ice-film surface will become smooth, even though the ice-water surface is rough. Surprisingly, the exponent dictating the transition does not depend on the thickness of the layer, as long as g'' is finite. Only the precise value of w is dictated by the premelting thickness [27].

Our theoretical approach explains our simulation results and is consistent with experimental observations. The roughening transition of the prismatic plane has been measured for ice crystals in water [53] and vapor [9,54]. It is found that from $\Delta T \approx -16$ K up to the triple point, the ice-water interface is rough, while, due to the limited width of the quasiliquid layer, the ice-film surface remains smooth up to $\Delta T \approx -4$ to -2 K, as suggested in our simulations. In fact, in the atmosphere ice crystals exhibit faceted prismatic faces up to 0 °C, even at very low saturation [2]. Since smooth surfaces have a slow activated dynamics, our results suggest it is the formation of the quasiliquid layer that could actually slow down the crystal growth rates and provide a mechanism for the change of crystal habits, as hypothesized by Kuroda and Lacmann [6].

In summary, we have shown that close to the triple point a quasiliquid layer of premelting ice on the primary prismatic face behaves as two independent ice-water and water-vapor surfaces at small wavelengths, but becomes smooth at long wavelengths. Our results may help rationalize the role of the premelting layer in the morphology of ice crystals.

E. S. and J. B. acknowledge financial support from EU Grant No. 322326-COSAAC-FP7-PEOPLE-2012-CIG and from the Spanish grant Ramon y Cajal. L. G. M acknowledges financial support from Project No. MAT-2014-59678-R (Ministerio de Economia y Competitividad).

J. B. and P. L. contributed equally to this work.

*Department of Physics, University of Durham, South Road, Durham DH1 3LE, United Kingdom.
†lgmac@quim.ucm.es

[1] Morphology of Crystals, edited by I. Sunagawa (Terra Scientific Publishing Company, Tokyo, 1987).
[2] K. G. Libbrecht, Rep. Prog. Phys. **68**, 855 (2005).
[3] H. R. Pruppacher and J. D. Klett, *Microphysics of Clouds and Precipitation* (Springer, Heidelberg, 2010).
[4] X. Y. Liu, E. S. Boek, W. J. Briels, and P. Bennema, Nature (London) **374**, 342 (1995).
[5] Y. Furukawa and J. S. Wettlaufer, Phys. Today **60**, No. 12, 70 (2007).
[6] T. Kuroda and R. Lacmann, J. Cryst. Growth **56**, 189 (1982).
[7] R. Lipowsky, Phys. Rev. Lett. **49**, 1575 (1982).
[8] J. G. Dash, A. W. Rempel, and J. S. Wettlaufer, Rev. Mod. Phys. **78**, 695 (2006).
[9] M. Elbaum, Phys. Rev. Lett. **67**, 2982 (1991).
[10] A. Lied, H. Dosch, and J. H. Bilgram, Phys. Rev. Lett. **72**, 3554 (1994).
[11] H. Dosch, A. Lied, and J. H. Bilgram, Surf. Sci. **327**, 145 (1995).
[12] H. Bluhm, D. F. Ogletree, C. S. Fadley, Z. Hussain, and M. Salmeron, J. Phys. Condens. Matter **14**, L227 (2002).
[13] G. Sazaki, S. Zepeda, S. Nakatsubo, M. Yokomine, and Y. Furukawa, Proc. Natl. Acad. Sci. U.S.A. **109**, 1052 (2012).
[14] K.-i. Murata, H. Asakawa, K. Nagashima, Y. Furukawa, and G. Sazaki, Phys. Rev. Lett. **115**, 256103 (2015).
[15] J. S. Wettlaufer, Phys. Rev. Lett. **82**, 2516 (1999).
[16] W. K. Burton, N. Cabrera, and F. C. Frank, Phil. Trans. R. Soc. A **243**, 299 (1951).
[17] J. D. Weeks and G. H. Gilmer, Adv. Chem. Phys. **40**, 157 (1979).
[18] C. Jayaprakash, W. F. Saam, and S. Teitel, Phys. Rev. Lett. **50**, 2017 (1983).
[19] C. Rottman and M. Wortis, Phys. Rev. B **29**, 328 (1984).
[20] P. M. Chaikin and T. C. Lubensky, *Principles of Condensed Matter Physics* (Cambridge University Press, Cambridge, England, 1995).
[21] J. L. F. Abascal and C. Vega, J. Chem. Phys. **123**, 234505 (2005).
[22] C. Vega and J. L. F. Abascal, Phys. Chem. Chem. Phys. **13**, 19663 (2011).
[23] M. Watkins, D. Pand, E. G. Wang, A. Michaelides, J. VandeVondele, and B. Slater, Nat. Mater. **10**, 794 (2011).
[24] V. Buch, P. Sandler, and J. Sadlej, J. Phys. Chem. B **102**, 8641 (1998).
[25] S. W. Rick and A. D. J. Haymet, J. Chem. Phys. **118**, 9291 (2003).
[26] L. G. MacDowell and C. Vega, J. Phys. Chem. B **114**, 6089 (2010).
[27] See Supplemental Material at http://link.aps.org/supplemental/10.1103/PhysRevLett.117.096101 for the model, simulation details, and theory, which includes Refs. [28–35].
[28] G. Bussi, D. Donadio, and M. Parrinello, J. Chem. Phys. **126**, 014101 (2007).
[29] K. Rommelse and M. den Nijs, Phys. Rev. Lett. **59**, 2578 (1987).
[30] N. Goldenfeld, *Lectures on Phase Transitions and the Renormalization Group* (Perseus Books, Reading, Massachusetts, 1992).
[31] L. G. MacDowell, arXiv:1512.04777.
[32] N. Akutsu, Y. Akutsu, and T. Yamamoto, Phys. Rev. B **64**, 085415 (2001).
[33] D. S. Fisher and J. D. Weeks, Phys. Rev. Lett. **50**, 1077 (1983).
[34] N. Akutsu and T. Yamamoto, in *Handbook of Crystal Growth (Second Edition)*, edited by T. Nishinaga (Elsevier, Boston, 2015), 2nd ed, pp. 265–313.
[35] J. Benet, L. G. MacDowell, and E. Sanz, J. Chem. Phys. **142**, 134706 (2015).
[36] J. Benet, L. G. MacDowell, and E. Sanz, J. Chem. Phys. **141**, 034701 (2014).
[37] D. Rozmanov and P. G. Kusalik, Phys. Chem. Chem. Phys. **13**, 15501 (2011).
[38] M. M. Conde, C. Vega, and A. Patrykiejew, J. Chem. Phys. **129**, 014702 (2008).
[39] C. L. Bishop, D. Pan, L. M. Liu, G. A. Tribello, A. Michaelides, E. G. Wang, and B. Slater, Faraday Discuss. **141**, 277 (2009).
[40] D. Pan, L.-M. Liu, B. Slater, A. Michaelides, and E. Wang, ACS Nano **5**, 4562 (2011).
[41] D. T. Limmer and D. Chandler, J. Chem. Phys. **141**, 18C505 (2014).
[42] W. Lechner and C. Dellago, J. Chem. Phys. **129**, 114707 (2008).
[43] E. Sanz, C. Vega, J. R. Espinosa, R. Caballero-Bernal, J. L. F. Abascal, and C. Valeriani, J. Am. Chem. Soc. **135**, 15008 (2013).

[44] J. Benet, L. G. MacDowell, and E. Sanz, Phys. Chem. Chem. Phys. **16**, 22159 (2014).
[45] S. A. Safran, *Statistical Thermodynamics of Surfaces, Interfaces and Membranes*, 1st ed. (Addison-Wesley, Reading, 1994).
[46] J. J. Hoyt, M. Asta, and A. Karma, Phys. Rev. Lett. **86**, 5530 (2001).
[47] R. L. Davidchack, J. R. Morris, and B. B. Laird, J. Chem. Phys. **125**, 094710 (2006).
[48] A. Härtel, M. Oettel, R. E. Rozas, S. U. Egelhaaf, J. Horbach, and H. Löwen, Phys. Rev. Lett. **108**, 226101 (2012).
[49] M. Müller and M. Schick, J. Chem. Phys. **105**, 8282 (1996).
[50] E. Chacon and P. Tarazona, J. Phys. Condens. Matter **17**, S3493 (2005).
[51] D. Nelson, T. Piran, and S. Weinberg, *Statistical Mechanics of Membranes and Surfaces* (Word Scientific, Singapore, 2004).
[52] S. Dietrich, in *Phase Transitions and Critical Phenomena*, edited by C. Domb and J. L. Lebowitz (Academic, New York, 1988), Vol. 12, pp. 1–89.
[53] M. Maruyama, J. Cryst. Growth **275**, 598 (2005).
[54] H. Asakawa, G. Sazaki, K. Nagashima, S. Nakatsubo, and Y. Furukawa, Cryst. Growth Des. **15**, 3339 (2015).